2014 IEEE International Conference on Robotics & Automation (ICRA)
Hong Kong Convention and Exhibition Center
May 31 - June 7, 2014. Hong Kong, China

Guiding Effects and Friction Modeling for Tendon Driven Systems

Jens Reinecke, Maxime Chalon, Werner Friedl and Markus Grebenstein
DLR - German Aerospace Center
Institute of Robotics and Mechatronics
Email: jens.reinecke@dlr.de

***Abstract*— This paper discusses tendon friction effects regarding guiding and material selection. In order to extract valuable information for designers of tendon driven systems, several experiments are conducted to investigate e. g. the intrinsic friction or sliding effect. The results are used to build an experimental friction model and to derive a set of guidelines. The mechanical designer can use the proposed models to anticipate the friction for a given tendon path. Additionally, the guidelines help the mechanical designer to systematically verify the numerous constraints involved in the design process of a tendon driven system.**

I. Introduction

The Institute of Robotics and Mechatronics of the DLR has build an advanced anthropomorphic system [1]. In this system, as well as other robot [2] the choice of a tendon driven system has been made. Its main advantages are the possibility of remote actuation, the small footprint and the small inertia.

Nonetheless, as with any transmission system, the anticipation of the friction properties is paramount to achieve an effective design. During the initial design phase, a prediction of the friction effects helps the designer to decide e. g. between a sliding surface or a pulley with bearing. Similarly, the influence of guiding conditions and their effect on the lifetime of a tendon allows to select the proper material combinations. Later on, the friction models can be used to implement active friction compensation mechanisms and, depending on the friction type, observers can be designed. The experience gained in designing and operating the Awiwi Hand[1] (Fig. 1a) and the DEXHAND (see Fig. 1b) proved that the usual models are insufficient. For advanced systems, e. g. the Awiwi Hand which is actuated using 38 tendons, more complex effects must be accounted for in order to understand the link between design choices and resulting friction.

Already in the late 80's, one of the first tendon driven robotic hands, the MIT/Utah hand [3], was using pulley guiding and several publications considered the modeling of the friction effects [4], [5], [6]. Most of the modeling analyzed existing systems and did not provide comparisons between several technical solutions. The focus was laid on the sheath friction [7], [8], [9] or the pulley with bearing friction [10] and did not consider other effects, such as intrinsic friction or plastic deformation. In [8] friction and viscoelastic effects of tendons sliding on curved pathways are identified and modeled precisely. A control strategy to compensate the nonlinear effects such as the hysteresis is proposed and experimentally demonstrated. The availability

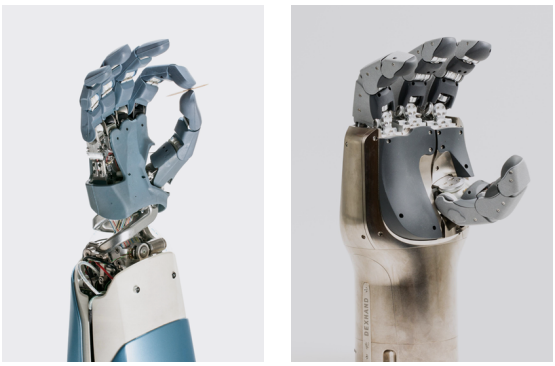

(a) DLR Hand Arm System (b) DEXHAND

Fig. 1: Examples of tendon driven hands at DLR

of many synthetic fibers as well as development of machining techniques offers many new options e. g. ceramic guiding. Only little work has been published on comparing material combinations [7] and guiding types. For the Awiwi hand, the Dyneema® [2] tendon was initially selected because of its superior durability and the possibility to splice it [11]. Steel tendons were discarded because they require large bending radii and are difficult to terminate on site [12]. Similarly, other fibers, such as Vectran, could not handle the small radii without a drastic reduction of their lifetime.

In this paper, multiple experiments are conducted to compare tendon materials, tendon paths, pulley shapes or load dependencies. As contribution the experimental results are used to formulate guidelines, helping the mechanical designers to select a technical solution. Additionally, a general model for tendon driven systems is computed, that helps to anticipate the friction behavior.

In the first section of the paper, the experimental setups are described and the results are reported. Each experiment focuses on key aspect, e. g. the load dependency. The second section discusses the results and proposes a general friction model. The third section formulates guidelines for the design of tendon driven systems.

[1]The Awiwi Hand is the hand of the Hand Arm System. Awiwi comes from the Hawaiian and means very fast.

[2]Dyneema® is a commercial name for a Ultra-high-molecular-weight polyethylene fibers

TABLE I: Hypothesis and Experiments

Experiment	Short Description	Detailed Description
I	The friction increases with the load	Sec. II-A
II	Friction due to the angle between the bending planes (at least 2 pulley)	Sec. II-B
III	Sliding friction with different material combinations	Sec. II-C
IV	Intrinsic friction of different material combinations	Sec. II-D
V	Pulley diameter dependent friction	Sec. II-E
VI	The friction dependent on the outgoing angle of a tendon from the pulley	Sec. II-F
VII	Influence of the pulley shape on the friction	Sec. II-G

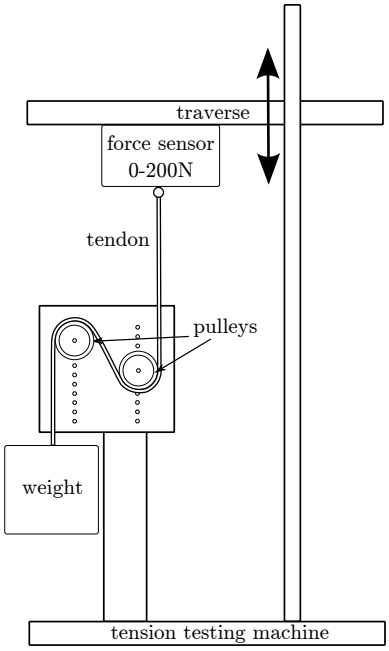

Fig. 2: Test setup for experiment I,III-V,VII

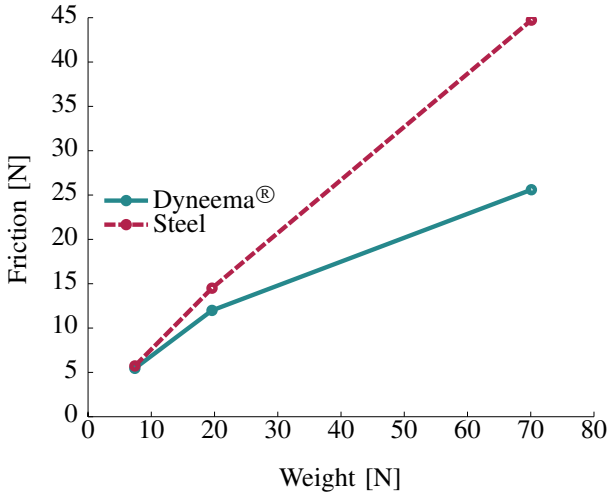

Fig. 3: Friction depending on the load. Green solid line: Dyneema® ; Red dashed: steel; both materials are tested on a PET joint material (ZX-100) of the Awiwi hand

II. Experiments description and results

This section describes the experiments used to verify hypothesis concerning the friction dependency of the tendons. All experiments were conducted on a Zwick tension testing machine (SN BZ1-MM14450.ZW01, [13]). A dedicated force sensor (200 N maximum, Zwick Xforce K, [14]) was used for the force measurement. The displacement was measured by the integrated incremental encoder of the testing machine. The setup is shown in Fig. 2. The view shows the pulling head of the tension testing machine, the tendon, the calibrated mass and the testbed. The testbed consists in a plate with several slots. Pulleys with bearings or fixed pulleys of different material, used for sliding experiments, can be placed on the slots in different configurations. Calibrated weights are used to impose a known loading condition. The testing machine pulls a tendon through the guiding with a load attached and the force as well as the head displacement are recorded. The conducted experiments are summarized in Table I.

A. Load

Motivation: The ranges of forces applied on each tendon varies for each finger in a robotic tendon driven hand. The maximum tendon force depends on the finger length, the coupling matrix [15] and the fingertip force. It is usually maximum for the thumb, since it has to oppose to the other fingers. The tendon force depends on the joint torque as well as the internal pretension. Indeed, in a nonlinear antagonistic setup, the stiffness can be adjusted by modifying the internal tendon forces. The choice of the stiffness should consider the friction introduced by the internal forces.

Setup description: The setup uses two fixed pulleys with the same surrounding angle. On the end of the tendon several calibrated weights are attached at the end of the tendon. Dyneema® and steel tendons are investigated. The difference between the expected load and the measured force gives the sliding friction depending on the load. The results are reported in Fig. 3. The sliding material used for the fixed pulley is the material used for the joints of the Awiwi finger.

Discussion: Dyneema® has less friction than steel on the polymer guiding used in this experiment. The steel has a linear behavior w. r. t. the load, whereas Dyneema® has a decreasing slope on higher loads. Below 20 N there is no significant difference between both materials, at higher load Dyneema® is superior. This experiment confirms that the weight has an influence. For the model only one μ for the working point of the DLR Hand Arm System is chosen.

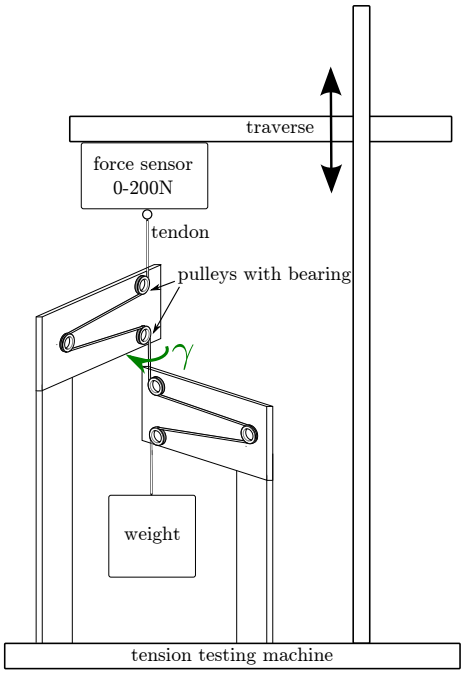

Fig. 4: The test setup consisting of two test plates, the green arrow shows the angle γ between the different bending planes

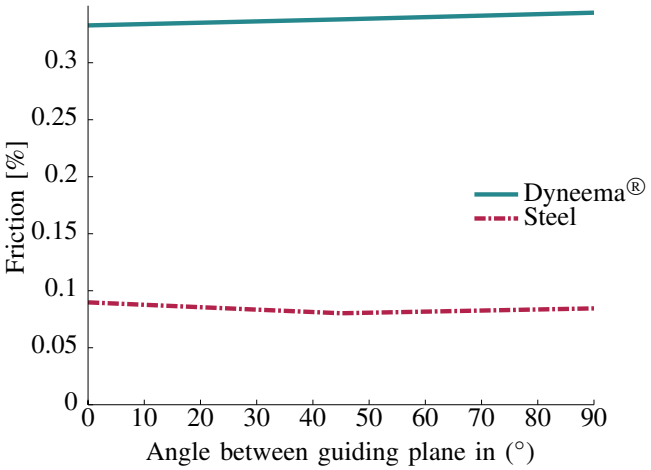

Fig. 5: Friction depended on the torsional angle γ ; Dark green line: Dyneema® on Aluminum alloy, Red dotted: Dyneema®

However, for the chosen material combination used in a tendon driven system, specific measurements should be used to create a model for the load dependency.

B. Angle between bending planes

Motivation: In the Awiwi hand a total of 38 tendons must be guided from the forearm through the wrist to the palm and then to the finger joints. The space available in the palm is restricted because the hand is human sized, implying that the tendons must be routed on several layers by pulleys placed freely in 3D space. The various distances between the pulleys imply that the tendon bending plane must change. The weaving of the tendon is following a spiral and consequently, the tendon torsion modifies tendon stiffness. The effect is called torsional friction in this paper.

Setup description: The torsional friction of Dyneema® and steel cables was experimentally measured with the setup depicted in Fig. 4. Two slotted plates, similar to the ones of the first experiment, can be fixed with an adapter to realize several angles between the bending planes. In this experiment the pulleys are placed on ball bearings. Because ball bearings have very low friction, it is possible to observe even small effects. It is expected that a high torsion angle results in higher friction, therefore the pulleys are placed as close as possible onto another.

Discussion: The forces reported in Fig. 5 prove that there is no discernible influence of the torsional friction. The force measured with or without torsion is not significantly different for the steel or the Dyneema® tendon. However, the metal tendon exhibits much lower friction compared to Dyneema® . The experiment in Sec. II-D will analyse this rarely modeled effect.

C. Sliding

Motivation: The use of a pulley with ball bearing for small bending angles requires a large volume and has to be replaced sometimes by a simple, and much more compact sliding surface. To be able to choose wisely between the two opportunities, the mechanical designer needs to have a comparison between the friction of bearing guiding and friction of sliding (Coulomb friction). Material science predicts that the sliding friction coefficient μ depends on tendon as well as the surface materials. The number of combinations between materials, loads and bending angles is exponentially increasing, therefore, the test are performed with a unique load and for only two angles. It is verified, according to mechanical science, that the bending angle or the load has no influence on the ranking of the materials.

Setup description: The experiment is conducted using a constant weight of 1.875 kg. The experimental procedure is similar to the one of the load dependency experiment. Two fixed pulley parts made of different materials: PVC, PET(ZX-100), aluminum-alloy, steel and ceramic are used in combination with Dyneema® , Dyneema® 2, Protec, Combat, Vectran and steel[3] tendons.

Discussion: The results for two surrounding angles are reported in Fig. 6. As expected, the bending angle does not influence the order. The friction of Dyneema® tendons is quite constant on every materials. The steel tendon has very high friction value on aluminum because the aluminum is soft and unlike the PVC, does not have a self lubricating behavior. The Dyneema® 2 tendon has the lowest friction on all materials. Vectran is one of the worst tendon, it is related

[3]The tendons are designed by their commercial names.

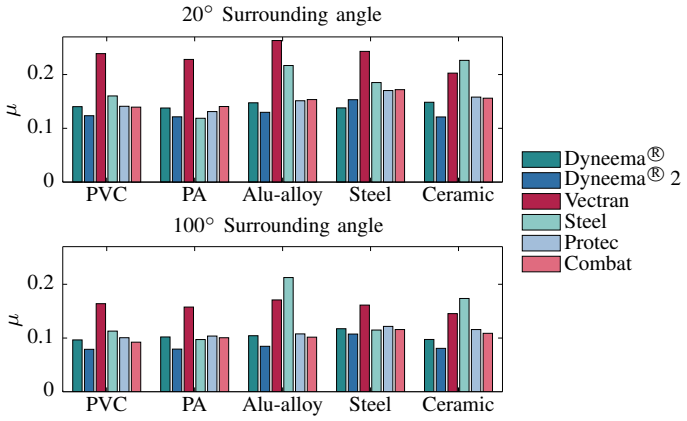

Fig. 6: Sliding experiments for a bending angle of 20 °and 100 °: friction coefficient for different material combinations. On the x-axis are different sliding materials.

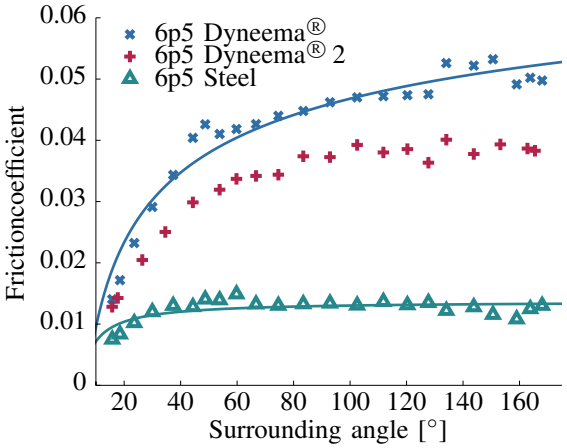

Fig. 7: Comparison of steel and Dyneema® tendons on friction generated at known surrounding angles

to its weaving type and its surface property. Steel tendons, combined with steel pulleys or joint material pulleys, exhibits a performance comparable to most of the polymer fibers.

D. Intrinsic friction

Motivation: The intrinsic friction that is related to the fiber material, as well as the tendon coating, is often neglected. It is rarely considered as an independent contribution to the friction. However, the torsion experiment highlighted its contribution to the overall friction. In a complex routing using polymer tendons, such as the one of the Awiwi hand, the intrinsic friction is the most significant part of the overall friction.

Setup description: The setup for this experiment is similar to the sliding setup. The main difference is that bearings are used, which allows to identify the intrinsic friction, since the ball bearing friction is known from the manufacturer. The friction is measured by varying the bending angle across a range from 10 °to 170 °.

Discussion: The graphs in Fig. 7 confirm the effect, which was visible in the torsional friction experiment. Steel has a lower intrinsic friction than the two Dyneema® types. As expected the uncoated Dyneema® has a lower intrinsic friction. In a long term testing, not reported herein, it is verified that, as the wax is degrading, the performance of the coated tendon approaches the one of the uncoated tendon. For each experiment a new tendon was used for each measurement point. If low friction is the objective steel tendons should be used, knowing that the lifetime is shorter and the maximum load is lower than with polymer tendons. An extra care should be given to design the mechanism, since steel tendons are more difficult to terminate. A comparable lifetime is achievable by using larger pulley diameters [12]. The shape of the curve is comparable to the ball bearing model proposed in [16], [17]. The amount of friction obtained with steel tendons is in accordance with ball bearing specifications [18], therefore it can be concluded, that steel tendons have negligible intrinsic friction.

E. Pulley Diameter

Motivation: The lifetime experiment in [12] showed, that the pulley diameter is a critical parameter. Therefore the influence of diameter is also tested concerning the intrinsic friction of the tendon. The results propose another parameter the designer can take into account. Obviously, a larger pulley diameter needs more space, but at the same time it could offer longer lifetime or reduced friction.

Setup description: The setup is similar as the one in the intrinsic friction Sec. II-D. Instead of several materials the pulley diameter is changed. Dyneema® has the highest intrinsic friction. In this experiment only Dyneema® was used, because the highest difference in the measurements of the friction are expected. For the diameter several pulleys (6.5-9.5 mm) were manufactured and placed on the same ball bearings. The diameters are chosen to start from the smallest size used in the tendon driven system available. The diameter is describing the core diameter of the tendon.

Discussion: Figure 8 depicts the dependency of the friction w. r. t. the bending angle. An obvious trend is observable, wherein an increase of friction on the tendon is related to a larger bending angle. A larger pulley generates a smaller intrinsic friction in comparison to a smaller pulley for an identical wrapping angle. This is because the bending of the tendon on larger pulleys is not as severe as that on smaller pulleys. This is due to the fact that the relative displacement of a core fiber w. r. t. a sink fiber is smaller if the pulley radius is larger.

F. Outgoing angle

Motivation: The palm routing requires the tendon to change directions several times. However, the space in an anthropomorphic sized tendon driven robot is limited (cf. Sec. II-B). Therefore, the designer has to decide to introduce

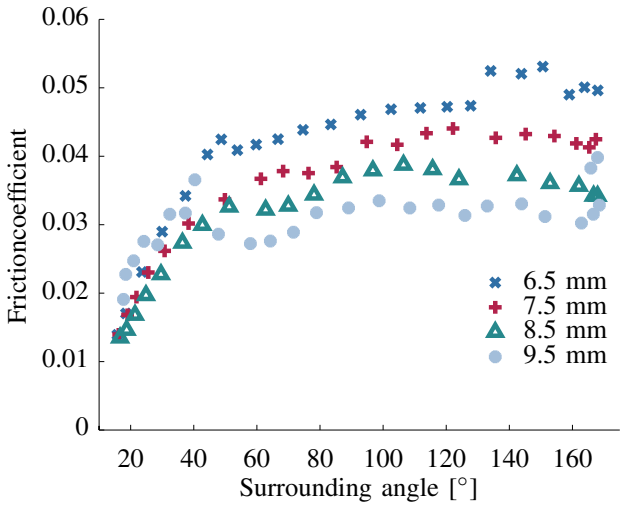

Fig. 8: Comparison of friction of Dyneema® on different pulley radius size from 6.5 mm to 9.5 mm

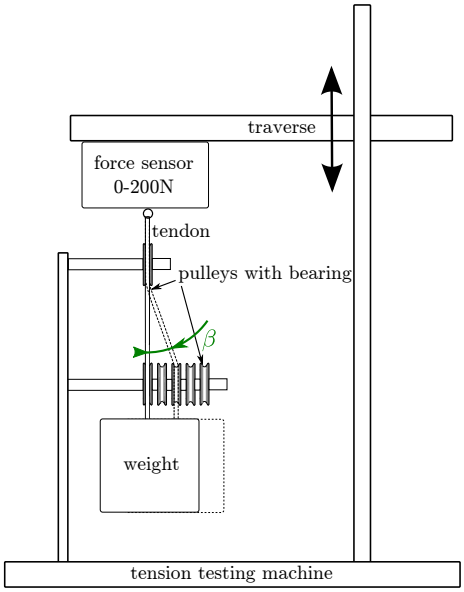

Fig. 9: Test setup of the outgoing measurement with the outgoing angle β

more pulleys or allow tendons to leave the pulleys out of their plane. Because each pulley needs a turning axes, it is expensive, in terms of space, to use numerous pulley planes. Close tendon paths can be grouped and routed using pulleys placed on the same turning axes, thus sparing important space. This approach can induce higher friction due to the sliding of the tendon on the pulley walls. Furthermore, a too large angle leads the tendon to jump out of the pulley. Several parameters such as the shape of the pulley or the surrounding angle influence the effects. The experiment uses pulley shape depicted in Fig. 12a.

Setup description: To achieve the same surrounding angle for each outgoing angle at least two pulleys have to be used.

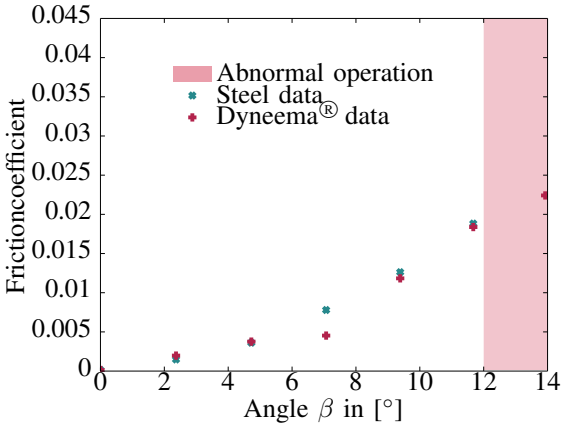

Fig. 10: Friction of steel and Dyneema® tendons dependent on the outgoing angle β, Crosses: Data points

The first one is guiding the tendon to a row of pulleys with an adjusted angle, such that the desired surrounding angle is achieved. The test consists in progressively increasing the outgoing angle by displacing the second pulley. The friction is again measured and it is also shown if the tendon jumps of the pulley. The pulleys have a diameter of 6.5 mm in that experiment and two materials are tested.

Discussion: The measurement of the friction of the outgoing angle show, that the relative friction is nonlinearly increasing with the outgoing angle. The experiment also gave information of the maximum outgoing angle. After 12°the tendon starts to jump of the bearing. This is also depending on the surrounding angle of the pulley. A higher surrounding angle is more stable against jumping of the tendon, because the length of the tendon, that is in contact with the pulley, is higher. As explained in the setup, a single surrounding angle that is representing the angle when changing the routing layer in the palm, is tested. Note that another surrounding angle can also change the friction, induced by the contact between tendon and pulley border walls.

G. Groove Shape

Motivation: The Dyneema® tendons are made of several polymer fibers that are braid together. The tendon shape flattens if it is guided on a pulley. Consequently, it is expected that the shape of groove of the pulley has an influence on the friction.

Setup description: For this experiment the test setup of the diameter change experiment is used. Instead of different pulley sizes the groove shape is varied. Figure 12 depicts the shapes used for the experiment. The weight is changed during the measurement between 2 kg and 7 kg. The first of the tested groove shapes in Fig. 12a is shaped according to the recommendation of the manufacturer of a steel tendons. The second shape, Fig. 12b, is a simple rectangular shape with round corners. The idea is to provide space for the tendon fibers to deform.

Discussion: Dyneema® has in both load cases slightly

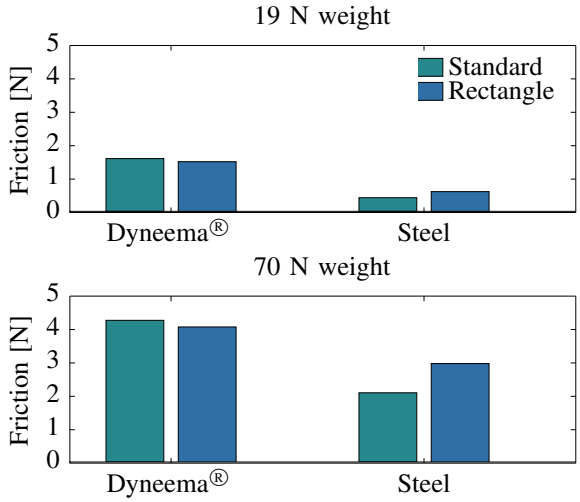

Fig. 11: Groove shape friction measurement for 19 and 70 N, two groove shapes, steel and Dyneema®

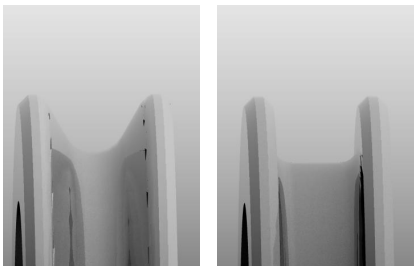

(a) Standard shape (b) Rectangle shape

Fig. 12: Pulley groove shapes

less friction than the standard pulley shape (cf. Fig. 12a). It highlights the influence of the groove shape. In contrast to the Dyneema® tendon, the steel tendon has less friction on the standard pulley, which emphasizes the importance of selecting the appropriate groove shape for a given tendon material.

III. Modeling

A model of the tendon friction for one tendon guiding path can be established from the experimental results. The friction is separated, in ball bearing, intrinsic, sliding and torsional bending friction. It is assumed that the relevant parameters are the surrounding angle, the outgoing angle, the torsion angle, loading force and the materials. It is important to note that the models are derived from experimental data and do not necessarily represent the underlying physical phenomenon. They are best suited for tendon driven hands or systems with very similar loading conditions. Therefore, extra care should be taken when extrapolating the results.

$$f_{t,fric}(\alpha,\beta,\gamma,f_{load}) = f_{t,bear} + f_{t,intr} \tag{1}$$

$$+ f_{t,slid} + f_{t,tors} + f_{t,outAngle}\,, \tag{2}$$

TABLE II: Model parameters of steel and dyneema with a working point of 20N and Aluminum alloy as sliding surface

(a) Steel

Parameter	Value
a	-0.3656
b	-0.7807
c	-0.05405
d	0.006247
f	0.1091
g	-0.006247
μ	0.1

(b) Dyneema

Parameter	Value
a	-5.387
b	-2.485
c	0.01212
d	0.0004002
f	0.3386
g	0.001116
μ	0.1

with α the surrounding angle. The force f_{load} is selected for the Awiwi working point around 20 N. The ball bearing friction an the intrinsic friction can not be measured separately in this experimental setup, thus the two components are implicitly modeled together. The different contributions add up and yield:

$$f_{t,pulley}(\alpha) = f_{t,bear} + f_{t,intr} = a(\alpha)^b + c\,. \tag{3}$$

The sliding friction drastically depends on the load. A simple model manages to capture the experimental data. The model is given by:

$$f_{t,slid} = f_{load}(e^{\alpha\mu} - 1)\,, \tag{4}$$

where μ is experimentally selected. The torsional friction $f_{t,tors}$ is neglected in this model, because the experiment demonstrated that it has no significant influence. The effect can become important if an another type of weaving or a different fiber material is used. In the case of the Awiwi one obtains:

$$f_{t,tors}(\beta) \approx 0\,. \tag{5}$$

The friction component related to the outgoing angle γ is expressed by:

$$f_{t,outAngle}(\gamma) = de^{f\gamma} + g\,. \tag{6}$$

The friction is increasing until the tendon jumps out of the pulley. Clearly, the model is only valid for angles below γ_{max}.

IV. Design guidelines

Unlike previous publications, the models are not concentrating on a specific technical solution but aim at comparing several approaches. The experiments and the models reported in the previous sections allow to derive a set a design guidelines. As often the guidelines can create contradictions and the designer has to realize the trade-offs.

- Steel tendons have less intrinsic friction, but at the same diameter of the tendon less maximum load force.
- The friction coefficients of certain material combinations, especially for small sliding angle, can be better than bearings.
- The intrinsic friction is reduced by using larger pulley diameter and less surrounding angle.

- Polymer tendons have the disadvantages of plastic deformation, which is critical if no link side sensors are used.
- Steel tendons have shorter life time than polymer tendons at equivalent pulley diameter.
- The torsional angle has negligible influence on the friction in the case of polymer and steel tendons.
- A harder sliding surface material lessens the friction in almost any material combination.
- A wax coating improves the tendon lifetime but increases the intrinsic friction.
- A polymer based tendon without wax coating is preferred, if the tendon path comprises mostly sliding surfaces.

V. Conclusion

This paper proposes an experimental modeling of several friction effects that were encountered during the development of the Awiwi hand. The guidelines are focusing on the loading condition that are representative of many tendon driven hands. The models provide aspects of tendon guiding that should be considered by the mechanical designer. The experimental data confirms the validity of the models. The work highlights the importance of some design parameters that are usually underestimated such as the groove shape or outgoing angle. The guidelines can be used as a checklist by the mechanical designer.

VI. ACKNOWLEDGEMENT

This work has been funded in parts by the European Commissions Seventh Framework Programme as part of the project The Hand Embodied (grant no. 248587). The authors are with the Robotics and Mechatronics Center (RMC), German Aerospace Center (DLR), Oberpfaffenhofen, 82234 Wessling, Germany

References

[1] M. Grebenstein, M. Chalon, W. Friedl, S. Haddadin, T. Wimböck, G. Hirzinger, and R. Siegwart, "The hand of the DLR hand arm system: Designed for interaction," *The International Journal of Robotics Research*, vol. 31, no. 13, pp. 1531–1555, 2012.

[2] A. Wedler, M. Chalon, and al., "DLRs space qualifiable multi-fingered DEXHAND," in *ASTRA*, 2011.

[3] S. Jacobsen, E. Iversen, D. Knutti, R. Johnson, and K. Biggers, "Design of the Utah/MIT dextrous hand," in *Robotics and Automation. Proceedings. 1986 IEEE International Conference on*, vol. 3. IEEE, 1986, pp. 1520–1532.

[4] A. Nahvi, J. Hollerbach, Y. Xu, and I. Hunter, "An investigation of the transmission system of a tendon driven robot hand," in *Intelligent Robots and Systems' 94.'Advanced Robotic Systems and the Real World', IROS'94. Proceedings of the IEEE/RSJ/GI International Conference on*, vol. 1, 1994, pp. 202–208.

[5] W. H. Rockenbeck, "Static load estimation using the utah/mit dextrous hand," Ph.D. dissertation, Massachusetts Institute of Technology, Department of Electrical Engineering and Computer Science, 1989.

[6] W. Townsend and J. Salisbury Jr, "The effect of coulomb friction and stiction on force control," in *Robotics and Automation. IEEE International Conference on*, vol. 4, 1987, pp. 883–889.

[7] G. Palli and C. Melchiorri, "Model and control of tendon-sheath transmission systems," in *Robotics and Automation, >IEEE International Conference on*, May,2006, pp. 988–993.

[8] G. Palli, G. Borghesan, and C. Melchiorri, "Modeling, identification, and control of tendon-based actuation systems," *Robotics, IEEE Transactions on*, vol. 28, no. 2, pp. 277–290, 2012.

[9] M. Kaneko and N. Imamaura, "Development of a tendon-driven finger with single pulley-type TDT sensors," *Intelligent Robots and Systems, IEEE International Conference on*, vol. 1, pp. 752–757, 1991.

[10] S. Uchiyama, J. Coert, L. Berglund, P. Amadio, and K.-N. An, "Method for the measurement of friction between tendon and pulley," *Journal of Orthopaedic Research*, vol. 13, no. 1, pp. 83–89, 2005.

[11] M. Grebenstein, M. Chalon, G. Hirzinger, and R. Siegwart, "Antagonistically driven finger design for the anthropomorphic DLR hand arm system," *Humanoid Robots, IEEE International Conference on*, vol. 1, pp. 609–616, 2010.

[12] W. Friedl, J. Reinecke, M. Chalon, and G. Hirzinger, "FAS A Flexible Antagonistic Spring element for a high performance tendon driven hand," *Intelligent Robots and Systems, IEEE International Conference on*, vol. 1, pp. 1366 – 1372, 2011.

[13] "Tensile testing maschine," Zwick, March 2013. [Online]. Available: http://www.zwick.de/fileadmin/content/gebrauchtmarkt/pdf/028976.pdf

[14] "Force sensor manual," Zwick, March 2013. [Online]. Available: http://www.zwick.de/de/produkte/xforce-kraftaufnehmer.html

[15] H. Kobayashi, K. Hyodo, and D. Ogane, "On tendon-driven robotic mechanisms with redundant tendons," *International Journal of Robotic Research*, vol. 17, no. 4, pp. 561–571, 1998.

[16] P. Dahl, "A solid friction model," The Aerospace Corporation, El Segundo, CA, Tech. Rep., 1968.

[17] ——, "Measurement of solid friction parameters of ball bearings," Tech. Rep., 1977.

[18] "Basic ball bearing application report," Rimpar, Tech. Rep., March 2013. [Online]. Available: http://www.grw.de/uploads/media/GRWGrundlagenKugellagerauslegung.pdf